The Film Thickness Effect on Electrical Conduction Mechanisms and Characteristics of the Ni–Cr Thin Film Resistor

**NAI–CHUAN CHUANG[1], JYI–TSONG LIN[1] (SENIOR MEMBER, IEEE),
TING–CHANG CHANG[2,3] (SENIOR MEMBER, IEEE), TSUNG–MING TSAI[4],
KUAN–CHANG CHANG[4], AND CHIH–WEI WU[5]**

1 Department of Electrical Engineering, National Sun Yat-sen University, Kaohsiung 804, Taiwan
2 Department of Physics, National Sun Yat-sen University, Kaohsiung 804, Taiwan
3 Advanced Optoelectronics Technology Center, National Cheng Kung University, Tainan 701, Taiwan
4 Department of Materials and Optoelectronic Science, National Sun Yat-sen University, Kaohsiung 80424, Taiwan
5 Walsin Technology Corporation, Kaohsiung 806, Taiwan

CORRESPONDING AUTHOR: N.-C. CHUANG (e-mail: ncchuang@passivecomponent.com)

ABSTRACT The electrical conduction mechanisms of Ni–Cr thin film resistor are demonstrated by different film thickness through scattering models fitting. The resistivity and temperature coefficient of the resistance of Ni–Cr thin film are measured to investigate the influence of thickness with different annealing temperature. Finally, an oxidation and atom inter-diffusion model was proposed to explain the effects of film thickness on the electrical properties of Ni–Cr thin film resistor under different annealing temperature.

INDEX TERMS Ni-Cr thin film, magnetron sputtering, conduction mechanism.

I. INTRODUCTION

With the demand of electronic devices increasing for telecommunication, information and wearable technologies, the logic device and passive component with high precision, reliability properties have become more important in the recent years. The function of resistor is to provide appreciate current and divide the voltage, from which resistor should have suitable stability against time and temperature variation. One of the important characteristics for resistors is low temperature coefficient of resistance (*TCR*) in electronic circuits [1].

In order to have high stability and low *TCR*, the thin film resistors are the most popular component in electronic circuits. Because the homogeneous resistive film is deposited by sputtering technology, many researches have been reported which focuses on resistive film's material composition and the sputtering and annealing conditions [2]–[9]. Typically a Ni-Cr alloy has been developed as resistive film for a thin film resistor, since it is provided with high electrical resistivity and low *TCR* performance [10]. The resistive characteristics of Ni-Cr thin film has been investigated and dominated by the resistive film thickness and annealing temperature [8]. The electrical properties of Ni-Cr is related to electron scattering mechanisms which corresponding to film thickness. However, a systematic research to determine the scattering mechanisms of carriers due to surface scattering, grain boundary scattering and surface roughness scattering in Ni-Cr films corresponding to electrical characteristics has not yet been reported to achieve reliable electrical and *TCR* characteristics.

A Ni-Cr thin film was prepared for a thin film precision resistor; resistivity complied with surface scattering was fitting by Sondheimer's model [11], grain boundary scattering and surface roughness scattering were fitting by the Mayadas-Shatzkes's model [12] and Namba's model [13], [14] respectively. The resistivity and *TCR* are measured to investigate the influence of different Ni-Cr thin film thickness after various annealing temperature. Finally, oxidation and atom inter-diffusion model are proposed to explain the effects of thin film thickness on the electrical properties of Ni-Cr thin film resistor.
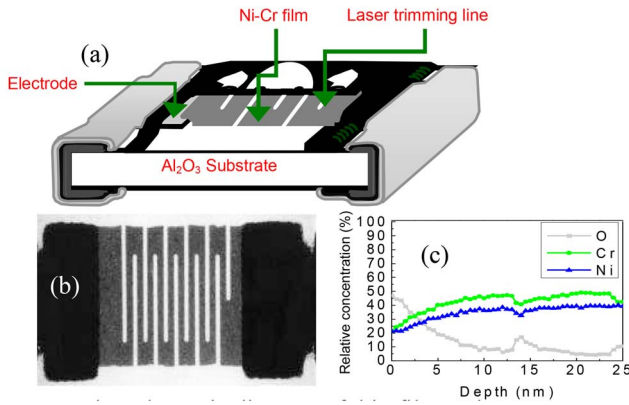
FIGURE 1. The schematic diagram of thin film resistor structure.

FIGURE 2. (a) The Sondheimer's model and (b) Mayadas-Shatzkes and Namba's models fit to Ni-Cr thin film resistivity data.

II. EXPERIMENTAL SETUP

The experimental thin film resistor devices shown in Fig. 1 (a) were prepared as follows: Firstly, the silver conductive material was printed on an alumina substrate. Then 10 to 200nm thickness of Ni-Cr thin film were deposited on the silver-printed substrate by DC sputtering. The concentration of Ni and Cr were about 1:1 by weight percentage analyzed by Auger electron spectroscopy (*AES*) as shown in Fig. 1 (c). After that all specimens were annealed in the temperature range of 250°C~450°C in nitrogen ambient for 5 hours. Then, the laser trimming process of Ni-Cr resistive film were done with serpentine pattern as shown in Fig. 1 (b) to obtain a specific

resistance value for electrical measurement. The *TCR* characteristics of thin film resistors were measuring the resistance using a digital multimeter (Hioki RM3542) at 125°C and room temperature, and were calculated using Equation (1):

$$TCR(ppm/^oC) = \{ (R_T - R_{25})/R_{25}(T - 25)\}x10^6 \quad (1)$$

where R_T and R_{25} are the film resistance measured at temperature 125°C and 25°C.

The thickness of the Ni-Cr thin film was measured using an N&K analyzer.

III. RESULTS AND DISCUSSION

A. ELECTRICAL CONDUCTION MECHANISM

The Mathiessen's rule assumes the scattering hypothesis for film resistivity. It must be considered that film surface and film-to-substrate interface scattering when the film thickness approaches the value of the electron mean free path (*MFP*). The Sondheimer's model for a continuous single crystalline film can be express as Equation (2) because the resistivity ρ is the ratio of *1/σ*:

$$\rho_f/\rho_o = \left[d + \frac{3\lambda}{8}(1 - P)\right]\frac{1}{d} \quad (2)$$

where ρ_f is the film resistivity and ρ_o is the bulk resistivity, λ is the *MFP* of the conduction electron and the value 24.2 nm for Ni-Cr thin film [15], d is the film thickness and P is the specularity coefficient of 0.1 to 1.
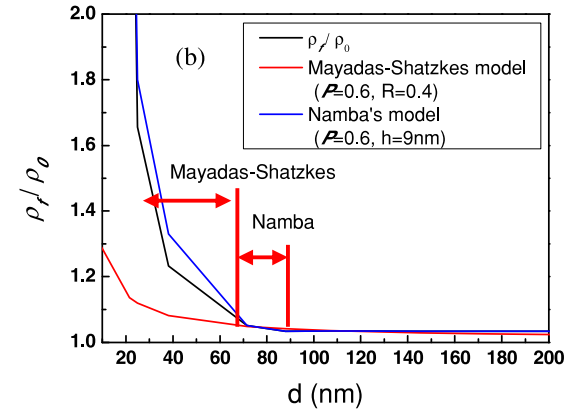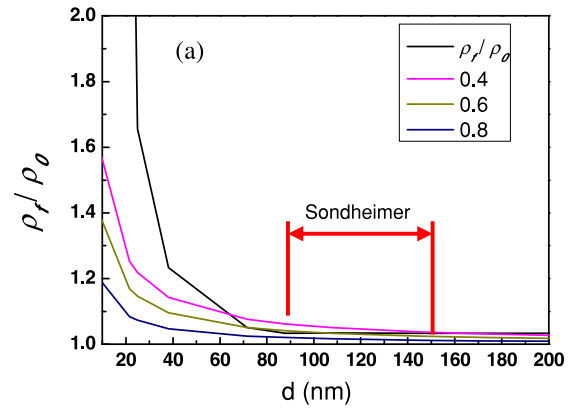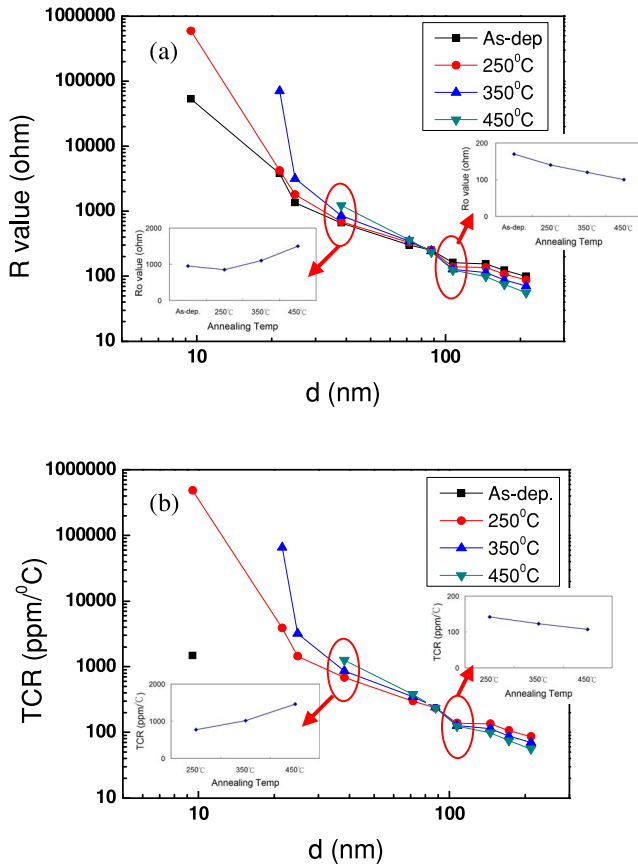
Fig. 2 (a) shows ρ_f/ρ_0 versus d data plotted in film thickness for $d < 200$ nm for the Sondheimer's mode given in Equation (2) by different values of the specularity parameter p. The film thickness $d > 90$ nm has the best match when $P = 0.6$ between the data and the theoretical model. This result proves that the other mechanisms must be considered because of the calculated resistivity does not match the data for $d < 90$ nm.

The Mayadas-Shatzkes's model of curves calculated is shown in Fig. 2(b) that given in Equation (3) with $P = 0.6$. When $R = 0.4$ and $\lambda / D = 0.85\lambda / d$ a better fit was found with the result as film thickness d was 65 nm to 90 nm. However, for film thickness $d < 65$ nm, the values are not matched to the resistivity result.

$$\rho_f = \frac{\rho_0}{3}\left[\frac{1}{3} - \frac{1}{2}\alpha + \alpha^2 - \alpha^3 \ln\left(1 + \frac{1}{\alpha}\right)\right]^{-1} \alpha = \frac{\lambda}{D}\frac{R}{1 - R} \quad (3)$$

The Namba's model results are also plotted in Fig. 2 (b). Besides the effect of surface and interface scattering, the surface roughness is correlated between the model and the resistivity result is achieved. The best fit was with the values of $p = 0.6$ and $h = 9$nm and the result of 9 nm is better

FIGURE 4. AES result of Ni-Cr film annealed at 350°C.

FIGURE 3. (a) The resistance and (b) TCR of different NiCr thin films thickness annealed at various temperature.

agreed with using Namba's model in Equation (4):

$$\rho_f = \rho_0 \left[1 - \left(\frac{h}{d}\right)^2\right]^{-\frac{1}{2}} + \rho_0 \frac{3\lambda}{8d}(1-\rho)\left[1 - \left(\frac{h}{d}\right)^2\right]^{-\frac{3}{2}} \quad (4)$$

The electrical conduction mechanism of scattering for Ni-Cr thin film can be summarized as follows:

The discontinuous film with high resistivity is for $d < 10$ nm.
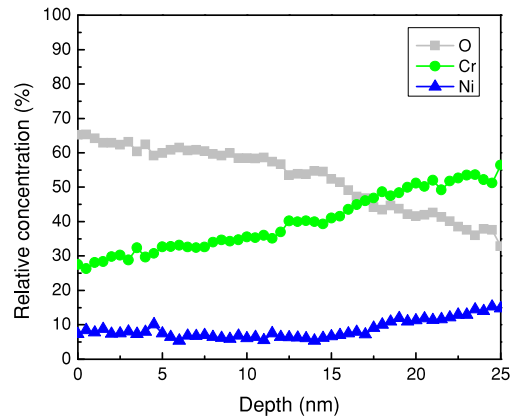
The surface roughness scattering is for $d = 10\sim65$ nm.

The grain boundary scattering is for $d = 65\sim90$ nm.

The surface scattering is for $d = 90\sim150$ nm.

The bulk conductivity is for $d > 150$ nm.

B. ELECTRICAL PROPERTY

Fig. 3 (a) shows the resistance of Ni-Cr film annealed at various temperatures for 5 hours in nitrogen ambient. In Fig. 3 (a), the resistance decreased with the increase in Ni-Cr film thickness of as-deposited film. After annealing process, the resistance increased with the increase in annealing temperature at a Ni-Cr film thickness thinner than 90 nm; when the Ni-Cr film thickness was thicker than 90 nm, the resistance was slightly decreased with the increase in annealing temperature. At Ni-Cr thin film is around 90 nm

thickness, the resistance is at fixed resistance value after various annealed temperature.

Fig. 3 (b) shows the *TCR* value of Ni-Cr thin films annealed at various annealing temperatures in nitrogen ambient for 5 hours. In Fig. 3 (b), when the thickness of the Ni-Cr film is less than 90 nm, the *TCR* increased with the increase in annealing temperature. When the thickness of the Ni-Cr film is thicker than 90 nm, the *TCR* decreased slightly with the increase in annealing temperature. At Ni-Cr thin film is around 90 nm thickness, the *TCR* value is at fixed value after various annealing temperature treatment.

As the thickness of Ni-Cr thin film is thinner than 90 nm, the as-deposited film is at island growth stage, after annealing process, the island film coalesced together and enlarged the distance of each island. Moreover, the oxygen can diffuse into the inter-space of island and oxide the thin film, leading to the resistance of Ni-Cr thin film increased. The electron transport between islands involves the hot electrons emission and acceptance through the barrier of the inter-island in the film. The scattering of electrons at imperfections is significant and strong dependent on temperature, so the *TCR* increased obviously.

As the thickness of Ni-Cr thin film is thicker than 90 nm, the as-deposited film is continuous film, the oxygen atoms entering into the Ni-Cr thin film was reduce and formed a Cr_2O_3 oxidation layer on the surface of Ni-Cr film during annealing process. The crystal grain combines to form a larger crystal grain. The surface area and the surface potential of the grain decreased, thus, the resistance of Ni-Cr film decreased. The *TCR* change was impacted by atom inter-diffusion in thin film. Fig. 4 shows the *AES* result of Ni-Cr film annealed at 350°C. The Cr_2O_3 oxidation layer is increasing after annealing process. The concentration ratio of Cr to Ni at surface is higher than the ratio of Cr to Ni of the as-deposited Ni-Cr film shown in Fig. 1 (c). This is because the Cr diffuse out to form Cr_2O_3 layer, then, Ni fill in the vacancies generated by Cr diffusion. This caused higher Ni concentration in the conductive layer. Thus, the *TCR* decreased with the increase in annealing temperature.
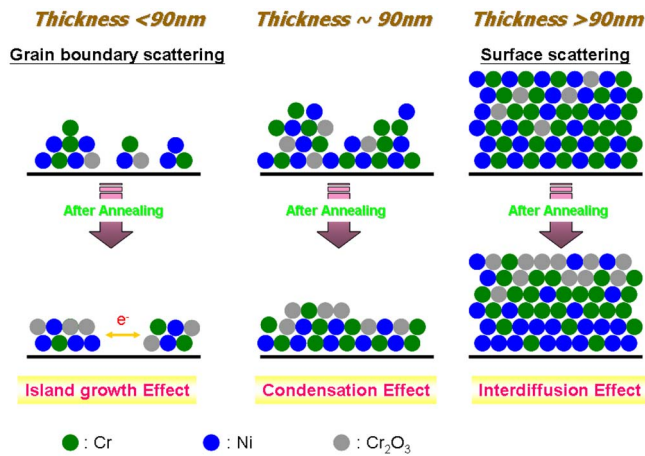
FIGURE 5. Conduction models of NiCr thin film with different thickness after annealing process.

As the Ni-Cr thin film is at around 90 nm thickness, the condensation effect was occurred. After annealing process, the Cr_2O_3 oxidation layer formed on the surface of Ni-Cr thin film and also the inner large grain forming, leading to resistance at a fixed value. The atom inter-diffusion in Ni-Cr thin film, the Ni atom is at a specific concentration due to Cr being diffused out and forming Cr_2O_3 under various annealing temperature, leading to *TCR* is at fixed value.

Base on the electrical analysis, the conduction models were proposed to explain the conduction mechanisms of Ni-Cr thin film with different film thickness (Figure 5). The oxidation and the atom inter-diffusion in Ni-Cr thin film can be controlled by different thin film thickness with various annealing temperature to achieve the *TCR* value equal to near-zero.

IV. CONCLUSION

Ni-Cr thin films with different thicknesses were fabricated using DC sputtering and annealed at different temperatures. The conduction scattering mechanisms of the surface roughness, grain boundary scattering and surface scattering were demonstrated relative to $d = 10\sim65$ nm, $d = 65\sim90$ nm and $d = 90\sim150$ nm, respectively. The resistivity and *TCR* of Ni-Cr thin film was measured. The results show that they were influenced by the thickness and the annealing temperature. The resistance and *TCR* increased with the increase in annealing temperature for Ni-Cr film thicknesses less than 90 nm. For film thicknesses thicker than 90 nm, the resistance and *TCR* decreased with the increase in annealing temperature. These phenomena were due to oxidation and the atom inter-diffusion in Ni-Cr thin films. Base on this model, it is believes that the near-zero *TCR* of Ni-Cr thin film resistor can be realized.

REFERENCES

[1] P. L. Kirby, "Applications of resistive thin films in electronics," *Thin Solid Films*, vol. 50, pp. 211–221, May 1978, doi: 10.1016/0040-6090(78)90107-4.

[2] Y. Q. Zhang, X. P. Dong, and J. S. Wu, "Microstructure and electrical characteristics of Cr–Si–Ni films deposited on glass and Si (1 0 0) substrates by RF magnetron sputtering," *Mater. Sci. Eng. B*, vol. 113, no. 2, pp. 154–160, 2004, doi: 10.1016/j.mseb.2004.07.086.

[3] Y. Sato, M. Watanabe, and S. Sato, "Electrical properties of Ni–Cr–N thin films deposited by multitarget reactive sputtering," *Jpn. J. Appl. Phys.*, vol. 40, no. 8, pp. 5091–5094, 2001, doi: 10.1143/JJAP.40.5091.

[4] N. M. Phuong, D.-J. Kim, B.-D. Kang, and S.-G. Yoon, "Structural and electrical properties of NiCr thin films annealed at various temperatures in a vacuum and a nitrogen ambient for π-type attenuator application," *J. Electrochem. Soc.*, vol. 153, no. 7, pp. G660–G663, 2006, doi: 10.1149/1.2202696.

[5] F. Wu, A. W. McLaurin, K. E. Henson, D. G. Managhan, and S. L. Thomasson, "The effects of the process parameters on the electrical and microstructure characteristics of the CrSi thin resistor films: Part I," *Thin Solid Films*, vol. 332, pp. 418–422, Nov. 1998, doi: 10.1016/S0040-6090(98)01042-6.

[6] M. Danisman and N. Cansever, "Effect of Cr content on mechanical and electrical properties of Ni–Cr thin films," *J. Alloys Compd.*, vol. 493, pp. 649–653, Mar. 2010, doi: 10.1016/j.jallcom.2009.12.180.

[7] I. H. Kazi, P. M. Wild, T. N. Moore, and M. Sayer, "The electromechanical behavior of nichrome (80/20 wt %) film," *Thin Solid Films*, vol. 433, pp. 337–343, Jun. 2003, doi: 10.1016/S0040-6090(03)00390-0.

[8] L. X. Zhao *et al.*, "The resistance characteristics of the Ni–Cr thin films and their influence on the integrated circuits," in *Proc. 5th Int. Conf. Solid State Integr. Circuit Technol.*, Beijing, China, 1998, pp. 123–126, doi: 10.1109/ICSICT.1998.785817.

[9] B.-J. Lee, S. W. Lee, and P.-K. Shin, "Precision thin film resistors based on Ni–Cr quinternary alloy thin films prepared by magnetron sputtering technique," *Jpn. J. Appl. Phys.*, vol. 48, no. 5, 2009, Art. no. 055502, doi: 10.1143/JJAP.48.055502.

[10] L.-F. Lai, X.-S. Su, X.-Z. Fu, R. Sun, and C.-P. Wong, "The microstructure and properties of C and W co-doped NiCr embedded thin film resistors," *Surface Coat. Technol.*, vol. 259, pp. 759–766, Nov. 2014, doi: 10.1016/j.surfcoat.2014.09.039.

[11] E. H. Sondheimer, "The mean free path of electrons in metals," *Adv. Phys.*, vol. 50, no. 6, pp. 499–537, 2001, doi: 10.1080/00018730110102187.

[12] A. F. Mayadas and M. Shatzkes, "Electrical-resistivity model for polycrystalline films: The case of arbitrary reflection at external surfaces," *Phys. Rev. B*, vol. 1, no. 4, pp. 1382–1839, 1970. [Online]. Available: http://dx.doi.org.ezproxy.lis.nsysu.edu.tw:8080/10.1103/PhysRevB.1.1382

[13] Y. Namba, "Resistivity and temperature coefficient of thin metal films with rough surface," *Jpn. J. Appl. Phys.*, vol. 9, no. 11, pp. 1326–1329, 1970, doi: 10.1143/JJAP.9.1326.

[14] H. D. Liu, Y.-P. Zhao, G. Ramanath, S. P. Murarka, and G.-C. Wang, "Thickness dependent electrical resistivity of ultrathin (<40 nm) Cu films," *Thin Solid Films*, vol. 384, no. 1, pp. 151–156, 2001, doi: 10.1016/S0040-6090(00)01818-6.

[15] N.-C. Chuang, J.-T. Lin, and H.-R. Chen, "TCR control of Ni–Cr resistive film deposited by DC magnetron sputtering," *Vacuum*, vol. 119, pp. 200–203, Sep. 2015, doi: 10.1016/j.vacuum.2015.05.026.

NAI-CHUAN CHUANG, photograph and biography not available at the time of publication.

JYI-TSONG LIN, photograph and biography not available at the time of publication.

TING-CHANG CHANG, photograph and biography not available at the time of publication.

TSUNG-MING TSAI, photograph and biography not available at the time of publication.

KUAN-CHANG CHANG, photograph and biography not available at the time of publication.

CHIH-WEI WU, photograph and biography not available at the time of publication.